Passive tracers and active dynamics – a model study of hydrography and circulation in the northern North Atlantic

C. Mauritzen[1], S. S. Hjøllo,[2] and A. B. Sandø[3]

1 – Norwegian Meteorological Institute, Oslo, Norway

2 – Bjerknes Centre for Climate Research, Bergen, Norway

3 – Nansen Environmental and Remote Sensing Center, Bergen, Norway

Corresponding Author:

C. Mauritzen,

Norwegian Meteorological Institute, Climate Division,

P.O. Box 43 Blindern,

0313 Oslo,

Norway.

e-mail: c.mauritzen@met.no

phone: +47 22 96 33 45

fax: +47 22 96 30 50

Abstract

A long-standing problem in oceanography has been to understand the relationship between what can be measured in the ocean, such as hydrography, and what cannot, such as the strength and structure of the *complete* Meridional Overturning Circulation (MOC) of the world oceans, commonly considered the main oceanic long-term modifier of Earth's climate. With the aid of a 50 year simulation from a numerical ice-ocean model we have investigated this relationship in the area of the northernmost extension of the MOC, in the Subpolar and Nordic Seas, on interannual timescales. We find that variability in the northward flux of salt and temperature in this region is controlled almost entirely by the volume flux, confirming that a knowledge of the variability of the circulation strength proper is necessary. The simulated hydrographic anomalies are within the range observed in the 20th century, thus fundamental changes to the circulation were not expected nor found. It is seen that variability in either temperature or salinity does contain some information about the variability in current strength, because hydrography and circulation generally respond to the same atmospheric forcing in the North Atlantic sector. Whether it is temperature or salinity that contains the information is related to the parameter range of the equation of state at the location in question: if density depends primarily on temperature then a salinity anomaly will tend to survive and vice versa. The oceanic response involves hydrographic changes and propagation of these, gyre strength changes, and changes in the MOC.

1. **Introduction**

It was proposed roughly half a century ago that ocean circulation could fluctuate between states due to the opposing effects temperature and salinity have on density (Stommel, 1961) and that it could even initiate an ice age (Ewing and Donn, 1956). Oceanic circulation and hydrography (temperature and salinity, which through the equation of state yields density) are inherently linked through the basic balance of the equations of motion: the geostrophic balance, which links horizontal density gradients to vertical velocity gradients[1]. They are also linked through buoyancy: water sinks if it is denser than the water beneath. It is the latter connection that gives rise to the possibility of an ice age: flushing of freshwater at the sea surface at northern latitudes would prevent the surface waters from becoming dense enough to sink, no matter how cold they are, thus shutting down the Meridional Overturning Circulation (MOC) of the North Atlantic, and therefore, hypothetically, shutting down the northward oceanic transport of heat, leading, hypothetically, to a significantly colder climate.

The last decades have indeed seen a significant change in the hydrography of the North Atlantic; the water masses have become less saline both in the Nordic Seas and in the Subpolar Gyre (Lazier, 1995; Turrell et al., 1999; Blindheim et al., 2000: Dickson et al., 2002, Curry et al., 2003), and the potential for abrupt climatic change due to changes in ocean circulation has been studied extensively (see e.g. Manabe and Stouffer (1988, 1995), Marotzke and Willebrandt (1991)). Recently, the amount of freshwater added to the North Atlantic during the last fifty years has been quantified (Curry and Mauritzen, 2005), revealing a gradual buildup of freshwater in the Subpolar Gyre equalling an addition of some 19.000

---

[1] Hydrography is easier to observe than ocean currents, so the geostrophic balance has been used extensively for almost a century to infer ocean velocities. However, basic inadequacies of the relationship are problematic: one obtains the velocity *shear* only, not the absolute velocity. In addition, the geostrophic balance does not always hold.

km^3 of freshwater, as well as certain periods when the buildup rate was much higher. These episodes have come to be known as "Great Salinity Anomalies" (GSAs). The largest of these, the GSA of the early 1970s was first described by Dickson et al. (1988). According to Curry and Mauritzen (2005) that GSA was associated with an accumulation of freshwater in the Subpolar Gyre of almost 0.1 Sv for a full five-year period in the 1970s. Later GSAs occurred in the 1980s and the early 1990s in the Subpolar Gyre (Belkin et al., 1998), but these were smaller in magnitude according to the Curry and Mauritzen (2005) quantification.

Although direct measurements of ocean circulation are sparse it is quite evident that a major change or shutdown of ocean circulation has not occurred in the North Atlantic during the last fifty years (not even in the 1970s) despite the significantly changing hydrography. We investigate here the relationship between hydrography and circulation *beneath* threshold levels, i.e. when the changes are not large enough to result in fundamentally altered circulation pathways (a switch in "regime", in Stommel's vocabulary). We focus directly on the northward flow of warm waters towards northern Europe and the Nordic Seas. At these high latitudes the MOC only partly represents the northward flow, because there is also a shallow return flow. Our goal is to gain further insight into the relationship between hydrography and the warm water currents towards the north, since we have measurements of the former for nearly a century, but much less information about the latter.

We do the work with the aid of a numerical model, due to the aforementioned sparse observational material. It is well known that numerical models in general struggle with simulating hydrography, so our results can be considered *suggestive* only. Nevertheless, we do know that this model has fared rather well in comparisons with observed hydrography (see e.g. Nilsen et al., 2003; Hátún et al., 2005a,b). The findings are further evaluated against

observations when possible. The paper is organized as follows: In section 2 the methods are presented. The model's hydrography and circulation are evaluated in sections 3.1 and 3.2, and its relationships between the two are discussed in sections 3.3 and 3.4. Finally the paper is summarized in section 4.

2. Methods

The model used is a nested version of the Miami Isopycnic Coordinate Ocean Model (MICOM) (Bleck et al., 1992), set up for the Nordic Seas and the northern North Atlantic (Figure 1). The nested model is initialized with interpolated model data from a global derivative of MICOM (Bentsen et al., 2004; Furevik et al., 2003; Nilsen et al., 2003). The global model has a resolution of about 40 km over most of the North Atlantic whereas the nested model has twice that resolution. Otherwise the grid configurations of the models are identical. The nesting approach applies a boundary relaxation scheme towards the outer (i.e. global) solution. This results in a so-called one way nesting where the boundary conditions of the nested model are relaxed towards the output from the global model. For the slowly varying baroclinic velocity, temperature, salinity and layer interface variables, this is a fully appropriate way to include the boundary conditions. For the barotropic variables, the relaxation approach requires careful tuning to avoid reflection of waves at the open boundaries. The nested model reads the global fields once a week and interpolates in time to specify the relaxation boundary conditions at each time step. In the vertical, both model versions have 26 layers of which the uppermost layer has temporal and spatial varying density, and the 25 layers below have constant density.

In the nested model, daily NCEP/NCAR re-analysis (Kistler et al., 2001) fresh water,

heat and momentum fluxes are used to force the system by applying the scheme of Bentsen and Drange (2000). If the model sea surface state is about equal to the assumed sea surface state of the NCEP/NCAR re-analysis data the turbulent fluxes of momentum and heat are estimated by the atmospheric model, which provides the re-analysis data. This model uses bulk expressions to estimate the turbulent fluxes with the coefficients determined by Miyakoda and Sirutis (1986). If the sea surface state differs significantly between the ocean model and the re-analysis data, the fluxes are modified.

Mixed layer temperature and salinity fields are linearly relaxed towards the monthly mean climatological values of Levitus et al. (1994) and Levitus and Boyer (1994), respectively. The e-folding relaxation time scale is set to 30 days for a 50 m thick mixed layer, and the relaxation is reduced linearly when the mixed layer depth exceeds 50 m. In addition, the relaxation is limited to a maximum difference between the observed and simulated sea surface salinity of 0.5 psu, and the observed and simulated sea surface temperature of 1.5°C. This constraint ensures that the hydrography in regions with large model biases, such as the region of the separation of the Gulf Stream system, is not destroyed by the applied relaxation. This all means that if no other forces or changes act on the waters, they would approach the relaxation target (i.e., monthly mean) salinity or temperature fields by a factor of 1/e after 30 days. However, the ocean surface waters are exposed to exchanges with surrounding waters and to daily atmospheric forcing in this period, so the effect of the relaxation will tend to be masked by atmospheric forcing, ocean transport and mixing processes.

Realistic runoff is incorporated through the NCEP/NCAR re-analysis data and the Total Runoff Integrating Pathways (TRIP) database (Oki and Sud, 1998), and the model is coupled to a sea-ice module consisting of the Hibler (1979) rheology in the implementation of Harder (1996) and the thermodynamics of Drange and Simonsen (1996). See further description of the model in Sandø and Drange (2005), and Hátún et al. (2005a).

The large-scale horizontal circulation is analyzed in terms of the vertically integrated stream function (Figure 2). We calculate the volume-weighted average temperature and salinity, as well as total heat- and freshwater content[2], in the upper 1000 m of the gyres, and calculate the different contents within each gyre as a function of time without correcting for volumetric changes. The Subpolar Gyre is defined by the 2000m isobath, except in south, where the mean position of the -12Sv stream function contour forms the boundary. We also calculate the size of the core of the Subpolar Gyre, because it is obvious that the core of the gyre contracts and expands significantly over time (Figure 2). To quantify that feature we calculate the area within a given streamfunction, here chosen as -24 Sv.

Changes in the Meridional Overturning Circulation are often studied by exploring the time variability of the maximum overturning in the North Atlantic (typically found at 40°N-50°N). This study is focussing on the variability at 60°-65°N, where one third of the total MOC enters the Nordic Seas across the Greenland-Scotland Ridge. Because the flow of light and dense water masses at these latitudes often are found in the same depth range we find it necessary to use a combination of temperature and density, rather than a depth interface, to differentiate between the northwardflowing warm water and the southwardflowing cold and

---

Heatcontent $H = \int c_p \rho_w (\theta - \theta_r) \, dz$ and freshwater content $F = \int (S_r - S)/ S_r \, dz$, where $c_p = 3990$ J kg^{-1}K^{-1}, $\rho_w = 1020$ kgm^{-3}, θ potential temperature, S salinity, $\theta_r = \theta_{1959-2002}$ and $S_r = S_{1959-2002}$.(i.e. averaged over the 1959-2002 period).

dense waters. In particular, we define the Norwegian Atlantic Current in terms of density and temperature, and calculate volume, temperature and salinity transports, as well as area-weighted temperatures and salinities of the Norwegian Atlantic Current for various sections along the coast of Norway (see Figure 1 and Table 1). In general we differentiate between warm Atlantic waters, cold Polar waters and dense overflows at the Greenland-Scotland Ridge.

All timeseries analyzed are annual means for the period 1959-2002 (the model itself was run for the period 1950-2002), and conclusions drawn are based on the occurrence of significant correlation coefficients between detrended time series. In calculating significance levels for correlations, the effective number of independent observations, adjusted for order 1 and 2 autocorrelations (N_e) were estimated by the formula of Quenouille(1952): $N_e = N/(1 + 2\, r_a^1\, r_b^1 + 2\, r_a^2\, r_b^2)$, where N is the number of data points in the two series (i.e. 43), r_a^1 and r_b^1 are the lag-one autocorrelations, r_a^2 and r_b^2 the lag-two autocorrelations. It is important to bear in mind that high correlation between two parameters can be due to either a close relationship between them *or* their simultaneous dependence on a third variable. Therefore any given correlation is only meaningful if it supports a scientific hypothesis.

3. Results

3. 1 Hydrography

The model has been evaluated against observations observed temperature (Hátún et al., 2005a) and salinity (Hátún et al., 2005b) at various locations near the Greenland-Scotland Ridge. In Hátún et al. (2005a) temperature observations from two different sections in the Faroe-Shetland Channel (Turrell et al., 2003) were merged to produce a century long hydrography time-series. The correlation between the 195 raw temperature observations and the

corresponding simulated temperature is was 0.93 without low-pass filtering, and 0.63 when annual averages were used. In addition, daily sea surface temperature measurements from Mykines on the south-western tip of the Faroes are available for the period 1 January 1914 to 18 September 1969. The correlation between the Mykines series and the simulated temperature anomalies on the Faroe Shelf was 0.96, and 0.75 when monthly averages were used. Hátún et al. (2005a) therefore demonstrate that both the simulated seasonal and interannual temperature variations on the Faroe Plateau are realistically captured by the model. In addition, the model simulates the observed changes in seasonal temperature variation both with respect to amplitude and phase. Therefore, Hátún et al. (2005a) demonstrate that the model is fully capable of simulating the interannual variability of the temperatures despite the applied temperature relaxation.

The same conclusion holds for interannual to decadal-scale variability of surface water salinity (Hátún et al., 2005b). In this study, observed and simulated salinities were compared in the Rockall Through, in the Irminger Sea and north of the Faroes. For all time series, a close match between the observed and simulated time series were obtained, again illustrating that the applied relaxation does not dampen hydrographic anomalies.

Finally, timeseries of the simulated top-to-bottom freshwater storage anomalies in the Subpolar Basins southward to 50°N show very similar freshening trend and interannual variability to that reported in observations (Curry and Mauritzen, 2005) for the last 40 years (Figure 3).

3.2 General circulation

3.2.1 General Circulation: Horizontal gyres

The large-scale model circulation is dominated by horizontal, cyclonic, gyres. The Subpolar Gyre has an average circulation strength of 40 Sv, whereas the Nordic Seas Gyre, has an average strength of 15 Sv (Figure 2a). During the fifty year model simulation the circulation strength varies substantially. For the Subpolar Gyre reaches a minimum in the early 1970, when the strength averaged ~35 Sv for five years (Figure 2b, core of gyre indicated by the thick contour line) and a maximum in 1994 of over 55 Sv (Figure 2d). This evolution in circulation strength is consistent, both qualitatively and quantitatively, with the transport index calculated by Curry and McCartney (2001), based on potential energy differences between the subpolar and subtropical gyres. The Nordic Seas Gyre reached a *maximum* of over 30 Sv in the early 1970s (Figure 2b) and a minimum of less than 10 Sv in the 1980s (Figure 2c). The amplitude of the variability in the gyres can thus be well over 50%. The *size* (defined as above)*,* in particular of the Subpolar Gyre, varies proportionally to the strength; a weaker Subpolar Gyre, such as around 1970, is narrower than a strong one, such as around 1995 (Figures 2b and 2d), thus the circulation strength changes are reflected in circulation pathway changes as well.

3.2.2 General circulation: inflow of warm Atlantic Water to the Nordic Seas

The MOC, bringing warm water northwards and dense, cold water southwards, is small in comparison to the gyres: At the southern boundary of the domain (30° N; where the MOC of the global model is imposed, see Figure 1) the MOC strength is roughly 18 Sv, and at the Greenland-Scotland Ridge the inflow of warm water to the Nordic Seas (defined as in Table 1) is on average between 6 and 7 Sv. The inflow of warm Atlantic Water at the Greenland-Scotland Ridge is distributed between the branch west and east of the Faroes: the Iceland-Faroe section carries roughly 2.5 Sv, and the Faroe-Scotland section carries nearly 4 Sv. The

contribution to the total inflow from the Irminger Current west of Iceland is small in comparison to the other two branches. These numbers are all consistent with observational evidence, which suggest that on average the former two branches carry around 3.5 Sv each, and the latter carries about $1/8^{th}$ of the total inflow (Kristmannsson, 1998, Hansen and Østerhus, 2000).

The model time variability of the exchange across ridge (Figure 4) is also less than that of the gyres: The warm-water inflow exhibits a minimum of 6 Sv in the mid-1960s followed by a maximum of 7.5 Sv in the early 1970s. Then the time series exhibits an all-time low of 5.5 Sv in 1980 and another maximum of 7.5 Sv around 1990. In relative terms, the variability of the northward flow of warm water across the Greenland-Scotland Ridge is roughly 15% of the mean.

3.2.3 General circulation: Return flow to the North Atlantic

The export of cold water back to the North Atlantic across the Greenland-Scotland Ridge is divided between dense waters overflowing the ridge and a flow of lighter Polar waters (defined as in Table 1). The dense overflow average about 2.3 Sv (Figure 4), and the light Polar waters, which return to the Atlantic in the same light density range as the northward flowing warm water, although much colder and much fresher, is generally as strong or stronger than that of the dense overflows (Figure 4). Comparing to the range of observations made on the Greenland-Scotland Ridge (see summaries in Hansen and Østerhus, 2000; McCartney and Mauritzen, 2001) it is clear that the model underestimates the strength of the dense overflows (compare the modelled 2.3 Sv to the observed ~5 Sv (Dickson and Brown, 1994)). The long-term average of the light outflows is less well known; Hansen and Østerhus

(2000) present numbers ranging from 1.3 Sv to 3 Sv, so the model's average 2.8 Sv is within the range of possibilities.

Both in the model, and in the real world, there is an imbalance in the volume flux across the Greenland-Scotland Ridge. This is possible because the system is not closed: it opens to the Arctic, and therefore to the Pacific Ocean through the Bering and to the Labrador Sea through the Canadian Archipelago. Observations at the Bering Strait indicate a 0.8 Sv net inflow from the Pacific to the Arctic Ocean (Woodgate and Aagaard, 2005). The net southward flow through the Canadian Archipelago is recently estimated to be 2 Sv (Prinsenberg and Hamilton, 2005). To be consistent with these observations there must be a net northward flow through the Nordic Seas, i.e. an imbalance between the northward and southward flow at the Greenland-Scotland Ridge, of roughly 1 Sv. This imbalance may be exaggerated in the model, because of the underestimation of the dense overflows.

During the 50 year simulation period the dense overflows varies by 20-30% on interannual timescales (Figure 4). There does not exist a significant relationship between the variability of the warm inflow and of the dense overflows. However, the *light* outflows (Polar waters of the East Greenland Current) are strongly correlated with the warm inflow, with no time difference (Figure 4). To summarize: Due to the Arctic throughflow there does not exist a one-to-one relationship between the strength of the northward flowing warm water and the southward flowing cold water across the Greenland-Scotland Ridge. In the model, variability in the warm inflow is strongly correlated (r=-0.62) with variability in the outflow of cold and light polar waters. No such relationship is found for the dense overflows. We cannot confirm whether this finding is robust, due to the underestimation of the strength of the dense

overflows. We do, however, find the result to be sensible, and it points to a possible decoupling of the upper limb of the MOC from the lower.

3.3 Hydrography and Circulation

3.3.1 Hydrography and Circulation: Subpolar Gyre

The time evolution of the freshwater content of the Subpolar Gyre is quite different if one considers only the upper part of the gyre rather than the full depth (which was discussed in section 3.1). In the upper part of the water column the salinity is characterized by interannual to decadal variability and a monotonic reduction of the freshwater content during the 1990s towards the saltiest waters of the simulation period (Figure 5; here the upper 1000m is used, but the finding is the same for the upper 200m or 500m). In particular, the observed salinity anomalies of the 1970s, 1980s and early 1990s in the Subpolar Gyre (see section 1) are reproduced.

The salinity anomalies are co-varying with temperature anomalies, such that when the Subpolar Gyre is fresh it is also cold (Figure 5). However, even though they affect density oppositely the density does not remain constant. Instead, the density follows the temperature evolution, giving the counter-intuitive result that when the Subpolar Gyre is fresh it is also dense (Figure 5). Observations from weather ship Bravo in the western Subpolar Gyre show the same result (Curry and McCartney, 2001).

Comparing the hydrography of the Subpolar Gyre to the circulation we find that increased strength of the Subpolar Gyre occurring during the periods of the "great salinity anomalies" (Figure 6). Specifically, these hydrographic anomalies are precursors of gyre circulation changes: About one year after the freshwater content of the Subpolar Gyre goes up the gyre

strength and width increases (Figure 6). We also note a second correlation: 5 years after the gyre strength and width goes up the freshwater content returns to normal. This points to an oscillatory nature of the phenomenon. Whereas the former correlation is limited to the upper waters, the latter is representative of the entire water column.

So can we establish a physical connection between these processes? Eden and Willebrand (2001) investigate the dynamic response of the Subpolar Gyre to atmospheric forcing, and describe it as a two-step process: First there is an immediate, barotropic, response (slowing down the gyre in the case of high NAO) driven by the winds alone, and then there is a delayed response (roughly 3 year lag time; speeding up the gyre in the case of high NAO) due to a combination of the wind and buoyancy forcing. Curry and McCartney (2001) emphasize the connection between the winter North Atlantic Oscillation index (NAO) and their baroclinic index of transport strength between the Subtropical and Subpolar Gyres; specifically they show the evolution from a low transport state in the 1970s to a high in the early 1990s. Häkkinen and Rhines (2004) show observational evidence for the decline in Subpolar Gyre strength in the 1990s (also seen in the model simulation, Figure 6) and relate it to changes in the buoyancy forcing over the Subpolar Gyre. So it is reasonable to hypothesize that the variability we have found in hydrography and circulation on interannual to decadal timescale is related to atmospheric forcing.

For simplicity we use the NAO index (specifically the December-March principal component based NAO data provided by the Climate Analysis Section, NCAR, Boulder, USA, see Hurrell, 1995) as a proxy for the large-scale atmospheric forcing. We could have picked a more sophisticated measure, but we believe the connections are well enough established through the use of the NAO. We find that an NAO increase is followed in the model by

hydrographic changes (cooling, due to the increased oceanic heat losses as more cold continental air reaches the western Subpolar Gyre, and freshening, due to increased freshwater export from the Arctic) in the upper waters of the Subpolar Gyre after about one year, by a strengthening and widening out of the Subpolar Gyre after 2 to 3 years, and, finally, by a warming and salinification in the entire water column after 7-8 years (Figures 6 and 7). This last response is not connected to the NAO (see Figure 7), which further suggests that it is symptomatic of an internal, oscillatory, response of the Subpolar Gyre.

In the Subpolar Gyre it is Eden and Willebrand's (2001) delayed, rather than immediate, response to the NAO we pick up in our analysis. As we will see in the next section, the model does exhibit an immediate response to the NAO, but it is found in the exchange across the Greenland-Scotland Ridge.

3.3.2 Hydrography and Circulation: Inflow of Atlantic water to the Nordic Seas

The inflow of Atlantic Water to the Nordic Seas across the Greenland-Scotland Ridge is fed by the North Atlantic Current, and draws upon waters both from the Subtropical and Subpolar Gyres. In their seminal paper on the "Great Salinity Anomaly", Dickson et al. (1988) describes how the anomalies propagate cyclonically from the western Subpolar Gyre towards the Greenland-Scotland Ridge and the Norwegian Atlantic Current. A recent study by Hátún et al. (2005b) investigates processes by which these anomalies occur.

At the Greenland-Scotland Ridge, the salinity evolution shows strong resemblance to that in the Subpolar Gyre (Figure 8), consistent with Dickson et al.'s (1988) observations. The salinity anomalies of the 70s, 80s and early 90s are present. As in the Subpolar Gyre the density anomalies at the ridge are controlled by the temperature evolution, not by the salinity

(Figure 9). In fact, salinity and temperature show a much stronger decoupling at the ridge than in the Subpolar Gyre (contrast Figures 9 and 5). Thus it follows that there is a clear relationship between the salinity anomalies of the Subpolar Gyre and those at the Greenland-Scotland Ridge (the latter lagging the former by less than a year; Figure 8), whereas the temperature anomalies in the two regions are not significantly correlated (not shown). There is a physical explanation for this: Since temperature is the dynamically active contributor to the vertical stability of the water column in both places, anomalies in temperature are quickly erased through buoyancy adjustment, whereas salinity anomalies can be passively advected with the general circulation, towards the ridge. These salinity anomalies can therefore maintain some memory of the forcing history.

Following this train of thought one can hypothesise that if there is some relationship between the atmospheric forcing in the Subpolar Gyre and the strength of the inflow of warm Atlantic Water across the Greenland-Scotland Ridge then there should be a relationship between salinity at the ridge and inflow strength across the ridge. And indeed this is found in the model: There exists a relationship between salinity and transport strength at the inflow, whereas no such relationship exists between temperature and transport (Figure 10). In the period two to four years after a transport increase in the inflow the salinity goes down. That is due to the following sequence of events:

- The inflow of Atlantic Water to the Nordic Seas across the Greenland-Scotland Ridge increases immediately in response to an increase in the NAO, as does the southward flow of light Polar water across the ridge (Figure 11).
- The hydrographic changes develop in the Subpolar Gyre after about one year (cooler, fresher, denser; Figure 7). The salinity anomalies advect eastward and appear at the Ridge quickly thereafter (Figure 8).

- The Subpolar Gyre starts spinning up and widening out 1-2 years thereafter (Figure 6). These dynamical changes to the Subpolar Gyre are not significantly correlated with the volume transport of warm water into the Nordic Seas. They are, however, as we have seen, correlated with the salinities at the ridge, in accordance with Hátún et. al (2005).

So salinity is an indicator of circulation change at the Greenland-Scotland Ridge, whereas temperature is not. However, due to the oscillatory nature of the salinity and inflow strength variability at the ridge (see symmetric correlations for $\pm$ 2 - 4 years in Figure 10), an oscillatory nature which is not imposed by the forcing (there is no such symmetry in Figure 11), one might claim that the salinity anomalies are indicators of circulation changes both earlier and later in time.

3.4 Norwegian Atlantic Current in the Nordic Seas and towards the Arctic

The flux of temperature into the Nordic Seas, which is important for maintaining the heat balance in that region, is generally dominated by the volume flux variability, not the temperature variability. The same is true for salinity. And this is true not only for the ridge region, but also for the series of sections along the coast of Norway shown in Figure 1. For all sections along the coast the correlation values between inflow and salt/temperature fluxes (Figure 12, lower panel) are higher than the correlation values between mean salinity/temperature and the same salt/temperature fluxes (Figure 12, upper panel). Observations support this finding: At the Svinøy section (our section no. 3), analysis of a record ten year observational timeseries has shown that on interannual timescales the

temperature flux is indeed dominated by the transport variability. It appears that only on longer timescales may temperature variability itself contribute significantly to the temperature flux (Orvik and Skagseth, 2005). This shows how important it is to monitor the circulation strength itself, to understand why it may change, and, optimally, to predict these changes.

The equation of state dictates that at lower temperatures, for instance in polar waters, the salinity becomes more and more influential for the density distribution. We see this in the model: As the Atlantic Water flows northward in the Nordic Seas and the temperature of the current drops, temperature loses some of its dominance over the density evolution; for instance at the Gimsøy section and at Barents Sea entrance, temperature and salinity contribute significantly to the density evolution (Figure 13, top). A complete switch to a salinity-controlled density distribution occurs as one reaches the Arctic (see the Fram Strait section in Figure 13, top). Because of this, and quite contrary to most other ocean basins, there exists a subsurface temperature maximum in the Arctic Ocean: The Atlantic layer. And because temperature is not the dynamically active partner in the Arctic it can be a passive tracer there, following the argument of the previous section. There are indeed numerous observations of temperature anomalies propagating cyclonically in the Arctic (see Quadfasel et al., 1991, Grotefendt et al., 1998).

In our model we see indications of a switch from a thermally to a haline-controlled density distribution starting around Gimsøy (Figure 13, upper panel). Following the idea that the passive tracer should carry some information about the forcing history, we should find a similar regime shift in the relationship between circulation and hydrography, and indeed we find a hint of this, albeit weak: South of Gimsøy the correlation between circulation strength and salinity is typically the strongest whereas at Gimsøy and northwards the correlation

between circulation strength and temperature is the strongest (Figure 13, lower panel). Observations at the Fram Strait entrance to the Arctic support this idea: Schauer et al. (2004) find a significant correlation there between a warm and a strong Atlantic Current. We repeat that these are weak correlations, and not always true (notably, at Rockall and the Faroe-Shetland section temperature is as strong an indicator of circulation change as salinity), but nevertheless they give yet another hint at what we set out to find: Relationships between hydrography and circulation.

4. Summary and Conclusions

With a numerical model we have investigated circulation and hydrography, and the relationship between the two, in the North Atlantic/Nordic Seas region, where the northernmost extension of the MOC extends beyond the Atlantic Ocean and continues towards the Arctic. Considering the technological difficulties in monitoring the strength of a current at a variety of locations it is not surprising that oceanographers seek to find relationships between current strength and oceanic variables that are more easily monitored, such as temperature and salinity. The time span of the simulation is fifty years, which is much too short to suggest robust statistical relationships. Nevertheless, this time span is comparable to the modern observational period, i.e. we do not have longer time series in the ocean without going to proxy data. Our findings are supported by a range of observational material, and the scenarios presented appear consistent. We should emphasize that the variability we have studied is of interannual to decadal nature. Our findings are of a general nature, i.e. they will obviously not always hold, not even in the model, but represent the most common occurrences.

We have shown that the northward temperature and salinity flux is controlled by the volume flux rather than the temperature and salinity of the current. We have also seen a connection between that volume flux and the hydrography. This is due to a common denominator: atmospheric forcing. I.e. the hydrographic anomalies are indicators of circulation change even though they are not the cause of it. We have established the following sequence of events:

- Atmospheric forcing (here condensed into the NAO index) increases in the Atlantic sector.

- The inflow of Atlantic Water to the Nordic Seas across the Greenland-Scotland Ridge increases immediately, as does the southward flow of light Polar water across the ridge.

- Hydrographic changes develop in the Subpolar Gyre after about one year (fresher, yet denser!). The salinity anomalies advect eastward and appear at the ridge quickly thereafter.

- The Subpolar Gyre starts spinning up and widening out 1-2 years thereafter. But these dynamical changes to the Subpolar Gyre have become de-correlated from the volume transport of warm water into the Nordic Seas.

This all leads to the interesting situation that the salinities of the northwardflowing MOC at the Greenland-Scotland Ridge are indicative of circulation strength changes in the northward flow of warm water across the ridge, in retrospect (2-4 years after the circulation change). The salinity anomalies originate in the Subpolar Gyre, and carry information about forcing – the same forcing that caused the circulation changes in the first place - as they propagate towards the ridge area. Due to a secondary, oscillatory, mode of variability in circulation and salinity at the ridge area the same salinity anomalies are also indicative of upcoming inflow changes 2-4 years afterwards.

Interestingly, even though temperature anomalies are just as prominent in the Subpolar Gyre as salinity anomalies are, they do not propagate towards the ridge area. In the hydrographic parameter range of the subpolar North Atlantic, temperature is the dynamically active contributor to density, and anomalies in temperature are therefore likely to be erased through buoyancy adjustment. Salinity, on the other hand, is free to passively advect, as has been observed in the North Atlantic repeatedly. This allows salinity to be an indicator of circulation change as described above.

Within the hydrographic parameter range of the Arctic the situation is the opposite: salinity is the dynamically active contributor to density. Here temperature can passively advect, as has been observed in the Arctic repeatedly. In the model the transition occurs around 70°N, north of which temperature also is an indicator of circulation change.

Salinity anomalies in the Subpolar Gyre occur due to local forcing, due to anomalies in the saline waters entering from the south, and due to unusually large pulses of freshwater and ice exported from the Arctic. As pointed out by Curry and McCartney (2001), even though these freshwater anomalies are dense anomalies, the introduction of freshwater lids can cause a cessation of dense water formation. Looking at the maximum overturning rate of the overturning in the North Atlantic (AMOC, rather than at the exchange across the Greenland-Scotland Ridge as we do in this paper), Häkkinen (1999) finds that its response depends strongly on where, when, and how fast the freshwater lid enters, and can be as large as 20%. Haak et al. (2003) find only minor responses in the AMOC as a result of salinity anomalies. Bentsen et al. (2004) show that AMOC responds 2-4 years after large (in the sense that both the Labrador and Irminger Seas are involved) variations in the atmospheric forcing. Clearly,

hydrographic anomalies play a multitude of roles in the North Atlantic, and in particular for the large circulation system we have come to appreciate as being fundamental to Earth's climate, the MOC.

Finally, our study suggests that it is important to consider the upper and lower limbs of the MOC separately, at least at these high latitudes, due to the possibilities of light returnflows and an exchange through the Canadian Archipelago (at lower latitudes the MOC may not have so many possibilities to disconnect). If one limits the definition of the MOC to that part of the northward flow which is needed to feed the dense return flows one reduces the problem, but loses a significant part of the current that brings warm water northward. European climate, to the extent that it is influenced by air-sea heat exchange in Atlantic sector, depends on the upper limb, not the lower limb, of the MOC. The lower limb of the MOC can of course have numerous other impacts on the dynamical couplings between ocean and atmosphere, but those are beyond the scope of this study.

References

Belkin, I.M., S. Levitus, J.I. Antonov, S.-A. Malmberg (1998), "Great Salinity Anomalies" in the North Atlantic, *Prog. Oceanogr.*, *41*, 1-68.

Bentsen, M. and H. Drange (2000), Parameterizing surface fluxes in ocean models using the NCEP/NCAR reanalysis data, *RegClim General Technical Report No. 4,* 149-158, Norwegian Institute for Air Research, Kjeller, Norway.

Bentsen, M., H. Drange, T. Furevik, and T. Zhou (2004), Simulated variability of the Atlantic meridional overturning circulation, *Clim. Dynam.*, *22*, 701-720.

Bleck R., C. Rooth, D. Hu, and L.T. Smith (1992), Salinity-driven thermocline Transients in a Wind- and Thermohaline-forced Isopycnic Coordinate Model of the North Atlantic, *J. Phys. Oceanogr.*, *22*, 1486-1505.

Blindheim, J. V. Borovkov, B. Hansen, S-A. Malmberg, W.R. Turrell, and S. Østerhus (2000), Upper layer cooling and freshening in the Norwegian Sea in relation to atmospheric forcing, *Deep-Sea Res. I*, *47*, 655-680.

Curry, R.G. and M.S. McCartney (2001), Ocean Gyre Circulation Changes associated with the North Atlantic Oscillation, *J. Phys. Oceanogr.*, *31(12)*, 3374-3400.

Curry, R., B. Dickson, and I. Yashayaev (2003), A change in the freshwater balance of the Atlantic Ocean over the past four decades, *Nature 426*, 826 – 829, doi:10.1038/nature02206

Curry, R., C. Mauritzen (2005), Dilution of the northern North Atlantic Ocean in recent decades, *Science*, *308* (5729), 1772-1774.

Dickson, R.R., J. Meincke, S.-A. Malmberg, and A.J. Lee (1988), The "Great Salinity Anomaly" in the northern North Atlantic, 1968-1982, *Prog. Oceanogr.*, *20*, 103-151.

Dickson, R.R., and J. Brown (1994), The production of North Atlantic Deep Water, sources, rates, and pathways, *J. Geophys. Res.*, *99*, 12319-12341.

Dickson, B., I. Yashayaev, J. Meincke, B. Turrell, S. Dye, and J. Holfort (2002), Rapid freshening of the deep North Atlantic Ocean over the past four decades, *Nature*, *416*, 832-837.

Drange, H., and K. Simonsen (1996), Formulation of Air-Sea Fluxes in the ESOP2 Version of MICOM, *Technical Report 125*, Nansen Environmental and Remote Sensing Center, Norway, Bergen, 23pp.

Eden, C., and J. Willebrand (2001), Mechanism of interannual to decadal variability of the North Atlantic circulation, *J. Climate*, *14*, 2266-2280.

Ewing, M., and W. L. Donn (1956), A Theory of Ice Ages, *Science*, *123*, 1061-1065.

Furevik, T., M. Bentsen, H. Drange, I.K.T. Kindem, G. Kvamstø, and A. Sorteberg (2003), Description and Validation of the Bergen Climate Model: ARPEGE coupled with MICOM, *Clim. Dynam.*, *21*, 27-51, doi:10.1007/s00382-003-0317-5

Grotefendt, K., K. Logemann, D. Quadfasel, and S. Ronski (1998), Is the Arctic Ocean warming? *J. of Geophys. Res.*, *103* (C12) p. 27679.

Haak, H., J. Jungclaus, U. Mikolajewicz, and M. Latif (2003), Formation and propagation of great salinity anomalies. *Geophys. Res. Lett.*, *30(9)*,1473,doi:10.1029/2003GL017065

Häkkinen, S. (1999), A simulation of thermohaline effects of a great salinity anomaly, *J. Climate*, *12*, 1781-1795.

Häkkinen, S. and P. B. Rhines (2004), Decline of Subpolar North Atlantic circulation in the 1990s, *Science, 304,* 555-559.

Hansen, B., and S. Østerhus (2000), North Atlantic-Nordic Seas exchanges, *Prog. Oceanogr.*, *45*, 109-208.

Harder, M. (1996), Dynamik, Rauhigkeit und Alter des Meereises in der Arktis, PhD Thesis, 124pp, Alfred-Wegener-Institut fur Polar- und Meeresforschung, Bremerhaven, Germany.

Hátún H., A.B. Sandø, H. Drange, and M. Bentsen (2005a), Seasonal to decadal temperature variations in the Faroe-Shetland inflow waters. In: *The Nordic Seas: an integrated perspective*, *Geophys. Monogr. 158,* editied by H. Drange, T. Dokken, T. Furevik, R. Gerdes, and W. Berger, AGU, Washington D.C.

Hátún H., B. Hansen, A.B. Sandø, H. Drange, and H. Valdimarsson (2005), Influence of the Atlantic Subpolar Gyre on the Thermohaline Circulation, *Science, 309,* 1841-1844

Hibler III, W.D. (1979), A Dynamic Thermodynamic Sea Ice Model. *J. Phys. Oceanogr.***,** 9, 815-846.

Hurrell, J. (1995), Decadal trends in the north atlantic oscillation: regional temperatures and precipitation, *Science, 269,* 676-679.

Kistler, R., Collins, W., Saha, S., White, G., Wollen, J., Kalnay, E., Chelliah, M., Ebisuzaki, W., Kanamitsu, M., Kousky, V., Van den Dool, H., Jenne, R., and Fionni, M. (2001), The NCEP-NCAR 50-Year Reanalysis, Monthly Means, CD-ROM and Documentation, *Bulletin of the American Society*, 82, 247-268.

Kristmannsson, S.S. (1998), Flow of Atlantic Water into the northern Icelandic shelf area, 1985-1989, *ICES Cooperative Research Report*, 225, 124-135.

Lazier, J.R.N. (1995), "The salinity decrease in the Labrador Sea over the past thirty years". In: *Natural climate variability on decade-to-century time scales*, edited by Martinson, D.G., K. Bryan, M. Ghil, M.M. Hall, T.M. Karl, E.S. Sarachik, S. Sorooshian and L. Talley, pp 295-302, National Academy Press, Washington D.C.

Levitus, S., Burgett, R., and Boyer, T.P. (1994), World Ocean Atlas 1994 Volume 3: Salinity, NOAA Atlas NESDIS 3, Washington, D.C., 99.

Levitus, S., Boyer, and T.P. (1994), World Ocean Atlas 1994 Volume 4: Salinity, NOAA Atlas NESDIS 3, Washington, D.C., 117.

Manabe, S. and R.J. Stouffer (1988), Two Stable Equilibria of a Coupled Ocean-Atmosphere Model, *J. Climate,* 1, 841-66.

Manabe, S. and R.J. Stouffer (1995), Simulation of abrupt climate change induced by freshwater input to the North Atlantic Ocean*, Nature*, *378*, 165-167.

Marotzke, J., J. Willebrand , 1991. Multiple Equilibria of the Global Thermohaline Circulation**.** *J. Phys. Oceanogr.,* 21(9), 1372–1385.

McCartney, M.S., C. Mauritzen (2001), On the origin of the warm inflow to the Nordic Seas. *Prog. Oceanogr.*, 51, 125-214.

Miyakoda, K. and J. Sirutis (1986), Manual of the E-physics. *Technical Report, Geophysical Fluid Dynamics Laboratory*, 72 pp, Princeton University, Princeton, New Jersey.

Nilsen, J.E.Ø., Y. Gao, H. Drange, T. Furevik, and M. Bentsen (2003), Simulated North Atlantic-Nordic Seas water mass exchanges in an isopycnic coordinate OGCM. *Geophys. Res. Lett.*, 30(10), 1536, doi:10.1029/2002GL016597.

Orvik, K. A., and Ø. Skagseth (2005), Heat flux variations in the eastern Norwegian Atlantic Current toward the Arctic from moored instruments, 1995-2005. *Geophys. Res. Lett.*, 32, L14610, doi:10.1029/2005GL023487.

Prinsenberg, S.J. and J. Hamilton (2005), Monitoring the volume, freshwater and heat fluxes passing through Lancaster Sound in the Canadian Arctic Archipelago, Atmosphere-Ocean, Vol.43(1):1-22.

Quadfasel, D.A., A. Sy, D. Wells, and A. Tunik (1991), Warming in the Arctic, *Nature*, 350, pp. 385.

Quenouille, M.H. (1952), Associated measurements. Butterworths, London, 241 pp.

Sandø, A. B. and H. Drange (2006), A nested model of the Nordic Seas. *Technical Report 268,* Nansen Environmental and Remote Sensing Center, Bergen, Norway.

Schauer U., E. Fahrbach, S. Østerhus and G. Rohardt (2004), Arctic warming through Fram Strait - Oceanic heat flow from three years of current measurements, *J. Geophys Res.,109*, C06026, doi:40.1029/2003JC001823.

Stommel, H. (1961), Thermohaline Convection with Two Stable Regimes of Flow, *Tellus 13*, 224-30.

Oki, T. and Y.C. Sud, Y. C. (1998), Design of Total Runoff Integrating Pathways (TRIP)—A Global River Channel Network, *Earth Interactions*, 2(1), 1-37.

Turrell, W.R., G. Slesser, R.D. Adams, R. Payne, and P.A. Gillibrand (1999), Decadal variability in the composition of Faroe Shetland Channel bottom water, *Deep-Sea Res. I*, 46, 1-25.

Woodgate, R.A., and K. Aagaard (2005), Revising the Bering Strait freshwater flux into the Arctic Ocean, Geophys. Res. Lett., 32, L02602, doi:10.1029/2004GL021747.

Turrell, W. R. , Hansen, B., Hughes, S., and Østerhus, S. (2003), Hydrodynamic variability during the decade of the 1990s in the Northeast Atlantic and southern Norwegian Sea, Marine Science Symposia, 219, 111-120.

Figure Captions

Figure 1: Map of the northern North Atlantic, including the Nordic Seas. Topography is
shaded within the model domain, and bottom contours are drawn for
500,1000,2000,3000,4000 and 8000m. Thick lines show sections for calculation of
model fluxes and mean values of salinity, temperature and density. 1) Rockall, 2)
Greenland-Scotland Ridge (GSR), 3) Svinøy, 4) Gimsøy, 5) Barents Sea opening and 6)
Fram Strait.

Figure 2: Upper 1000m vertically integrated stream function [Sv], averaged for the period a)
1960 to 2002, b) 1968-1972, c) 1983-1987 and d) 1993-1997. Also shown in figure a)
are the Subpolar Gyre (SPG) and Nordic Sea Gyre (NSG). The Subpolar Gyre is defined
by the 2000m isobath, except in south, where the mean position of the -12Sv stream
function contour forms the boundary. The Nordic Sea Gyre is defined as within the
2000m isobath and two straight lines between Jan Mayen (71°N,8°W) and Spitsbergen
(76°N,16°E) or Halten Bank (68°N,2°E). Contour interval is 5 Sv. In figure b-d), the
Subpolar Gyre *core* size is indicated by highlighting the -24Sv contour.

Figure 3: Timeseries of top-to-bottom freshwater content anomaly [10^3 km^3], relative to the
1959-2002 period, in the Subpolar Gyre, as defined in figure 2a.

Figure 4: Time series of volumetric exchange across Greenland-Scotland Ridge. The section
is indicated in Figure 1. The thick solid line shows northward transport of Atlantic
Water (positive northwards), defined as water warmer than 2°C and with potential
density (σ_0) less than 27.77 kg/m^3. The thick stippled line is dense overflow (σ_0>27.77
kg/m^3; θ<2°C), thin stippled cold, light outflow (σ_0<27.77 kg/m^3; θ<2°C). The thin
solid line is the sum of the two latter, and represents the sum of all southward flow
across the Greenland-Scotland Ridge. The imbalance between the thick and thin solid
lines represents northward flow into the Arctic.

Figure 5: a) Timeseries of non-dimensionalized average potential density anomaly (thick
solid), average salinity anomaly (thin solid) and average temperature anomaly (stippled)
in the Subpolar Gyre. Note that density anomaly is inverted. b) Correlations density vs.

salinity (solid) and density vs. temperature (stippled). Significance levels for the two curves are calculated separately (Quenouille, 1952), and may differ slightly. For simplicity, only the lowest value (strongest criteria for significance) is plotted (horizontal lines). Thus values between the lines are not significant. Negative time lag indicates that the first variable (here: potential density anomaly) leads the others (here: salinity and temperature anomalies). All timeseries are detrended before correlation.

Figure 6: a) Timeseries of non-dimensionalized upper 1000m freshwater content anomaly (FC) (thick solid), gyre width anomaly (thin solid) and gyre strength anomaly (stippled) in the Subpolar Gyre. b) Correlations freshwater content vs. gyre width (solid) and freshwater content vs. gyre strength (stippled). Otherwise as in Figure 5.

Figure 7: a) Timeseries of NAO index, non-dimensionalized freshwater content anomaly (solid) and gyre strength anomaly (stippled) in the Subpolar Gyre. b) Correlations NAO vs. freshwater content (solid), NAO vs. gyre strength (stippled). Otherwise as in Figure 5.

Figure 8: a) Timeseries of non-dimensionalized average salinity anomaly within the warm water inflow at the Greenland-Scotland Ridge (thick line) and in the Subpolar Gyre (thin line). b) Correlations average salinity in inflow vs. gyre. Otherwise as in Figure 5.

Figure 9: a) Timeseries of non-dimensionalized average density anomaly, (thick solid), average salinity anomaly (thin solid) and average temperature anomaly (stippled) for the warm water inflow at the Greenland-Scotland Ridge. Note that density anomaly is inverted. b) Correlations density vs. salinity (solid), density vs. temperature (stippled). Otherwise as in Figure 5.

Figure 10: a) Timeseries of non-dimensionalized volume transport anomaly (thick solid), average salinity anomaly (thin solid) and average temperature anomaly (stippled) for the warm Atlantic Water inflow at the Greenland-Scotland Ridge. b) Correlations transport vs. salinity (solid), transport vs. temperature (stippled). Otherwise as in Figure 5.

Figure 11: a) Timeseries of NAO index, non-dimensionalized warm Atlantic Water inflow (solid) and cold, light Polar Water outflow (stippled) anomalies at the Greenland-

Scotland Ridge. b) Correlations NAO vs. warm inflow (solid), NAO vs. Polar outflow (stippled). Otherwise as in Figure 5.

Figure 12: Absolute value of correlation between a) average salinity and salt flux (circles) or average temperature and temperature flux (triangles) and b) circulation and salt flux (circles) or circulation and temperature flux (triangles). Time lag indicated at right of symbol if present. Time series are detrended before correlation, and significant values according to Quenouille(1952) are shown by bold figures.

Figure 13: Absolute value of correlation between a) density and salt (triangles) or temperature (circles) and b) circulation and salt (triangles) or temperature (circles). Time lag indicated at right of symbol if present. Time series are detrended before correlation, and significant values according to Quenouille(1952) are shown by bold figures.

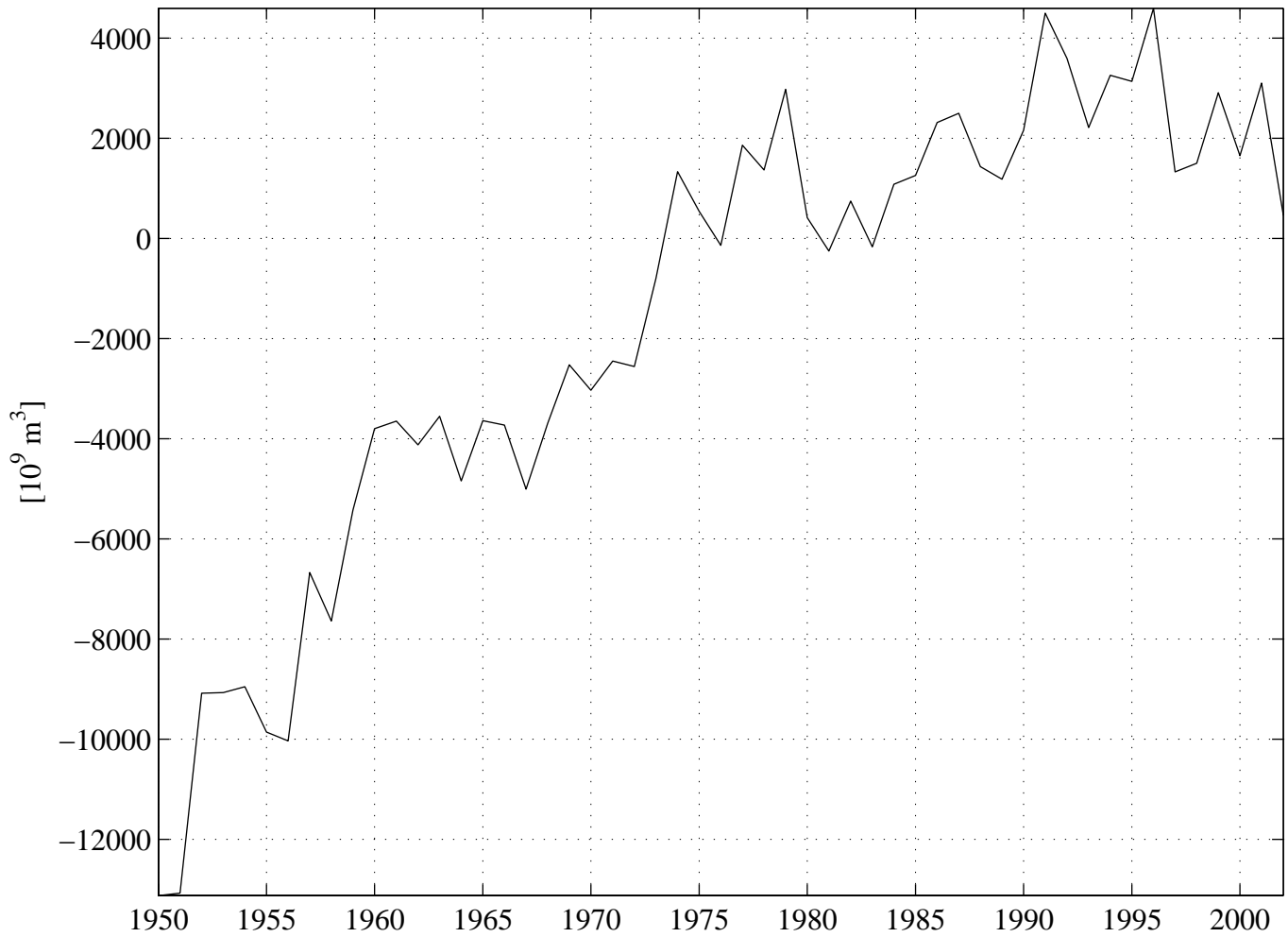**Table 1: The water mass definitions used in transport calculations**

Section name	Watermass definitions	Mean transport of			Mean	
		Volume [Sv]	Heat [TW]	Salt [kT/s]	S [psu]	θ [°C]
Rockall (1)	Atlantic Water σ_θ <27.38 kgm^{-3}	6.1	234	221	35.28	9.7
Iceland-Faroe	Atlantic Water σ_θ <27.77 kgm^{-3} θ >2°C	2.6	75	90	35.05	7.1
Faroe-Scotland	Atlantic Water σ_θ <27.77 kgm^{-3} θ >2°C	3.8	142	139	35.22	8.5
Svinøy (3)	Atlantic Water σ_θ <27.77 kgm^{-3} θ >2°C	6.6	199	245	35.01	6.9
Gimsøy (4)	Atlantic Water σ_θ <27.77 kgm^{-3} θ >2°C	7.1	179	258	34.93	5.9
Barents Sea opening (5)	Atlantic Water σ_θ <27.77 kgm^{-3} θ >2°C	2.8	55	109	34.87	4.3
Fram Strait (6)	Modified Atlantic Water σ_θ <27.98 kgm^{-3} θ >0°C	-0.5	-2	-18	34.81	0.7
Greenland-Scotland Ridge (2)	Atlantic Water σ_θ <27.77 kgm^{-3} θ >2°C	6.7	224	241	35.01	7.4
Greenland-Scotland Ridge (2)	Light Polar Water σ_θ <27.77 kgm^{-3} θ <2°C	-2.8	-13	-96	34.08	-1.2
Greenland-Scotland Ridge (2)	Dense Overflow Water σ_θ >27.77 kgm^{-3} θ <2°C	-2.3	-3	-81	34.80	-0.2

Table 1. Mean values (1959-2002) of volume, heat and salt transport, and temperature and salinity in the Atlantic water mass layers of sections 1-6 in figure 1. For section 2, the Greenland-Scotland Ridge, mean values for the cold out-flowing water mass layers also are shown. The section is divided into the Iceland-Faroe and Faroe-Scotland part as well. σ_θ is potential density, T temperature and S salinity. Transport is net transport, directed northward, and 1 Sv=10^6 m^3/s.
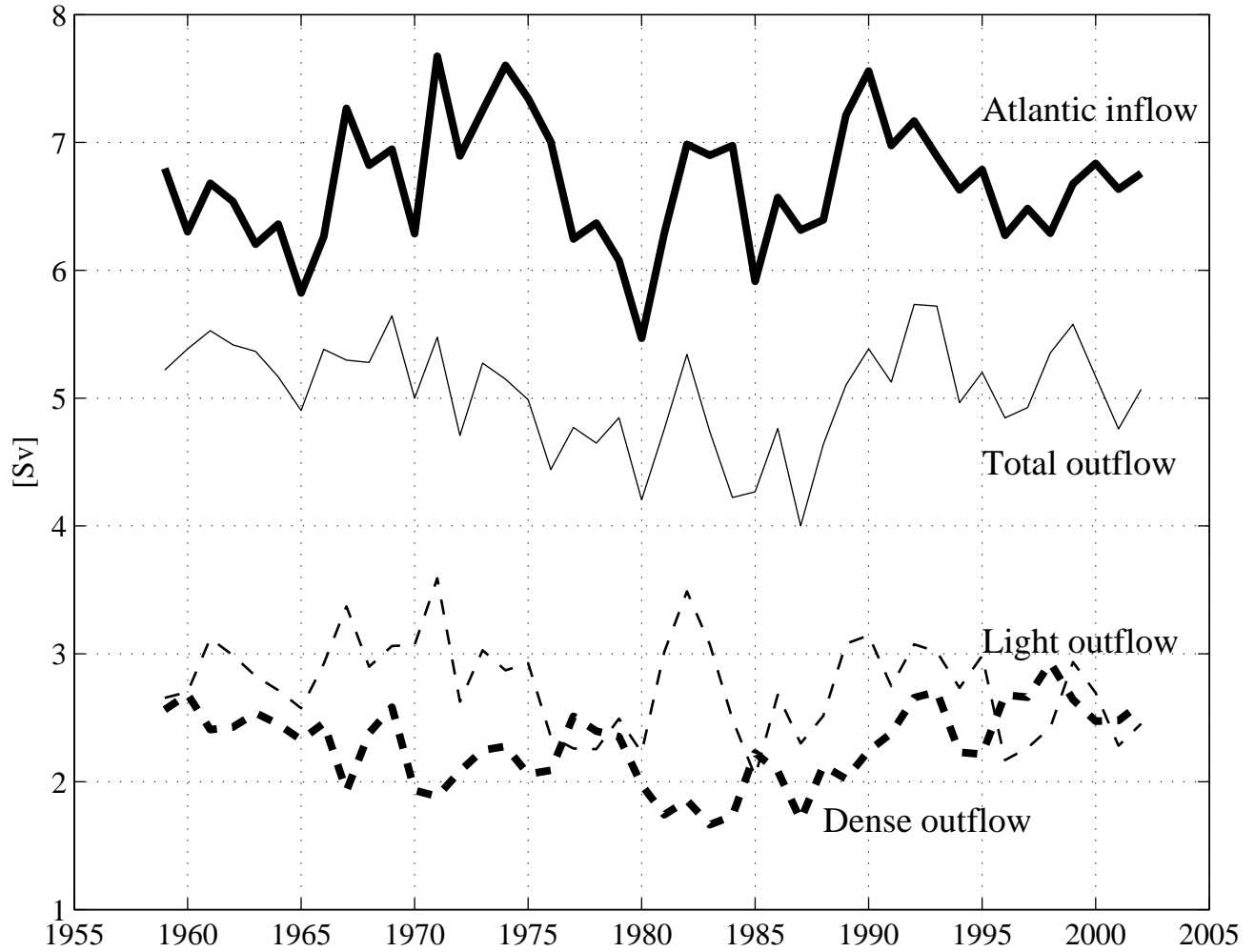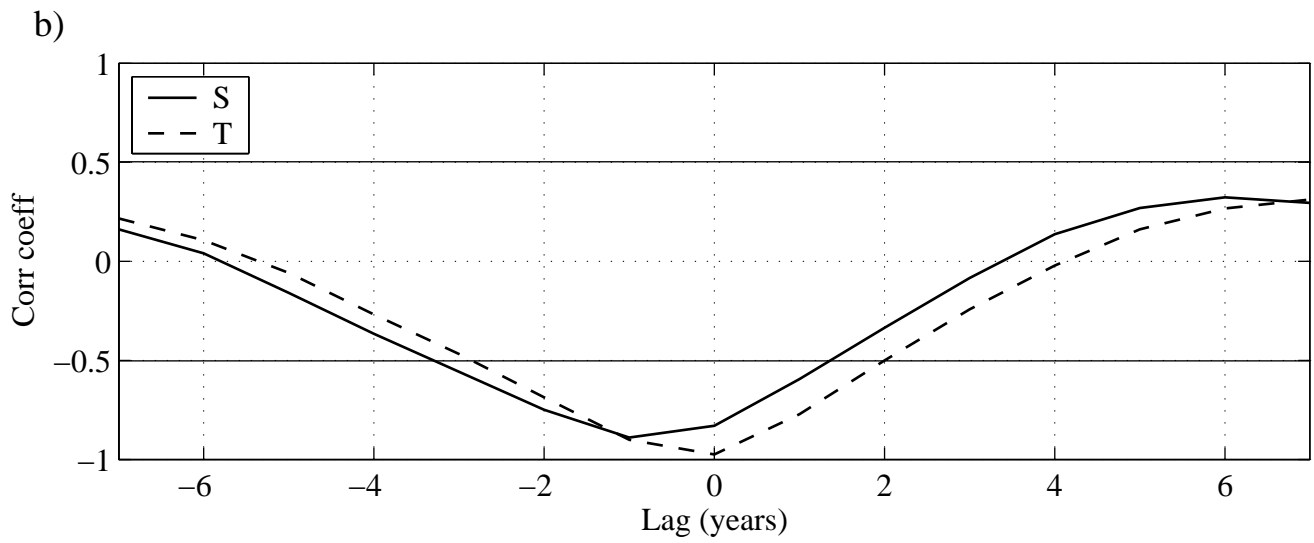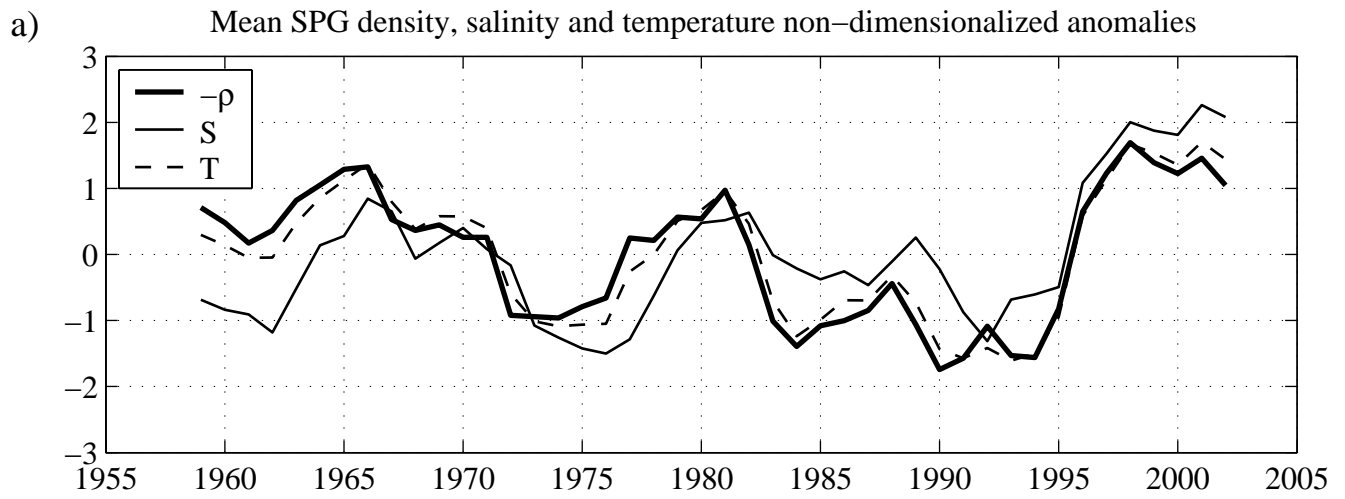
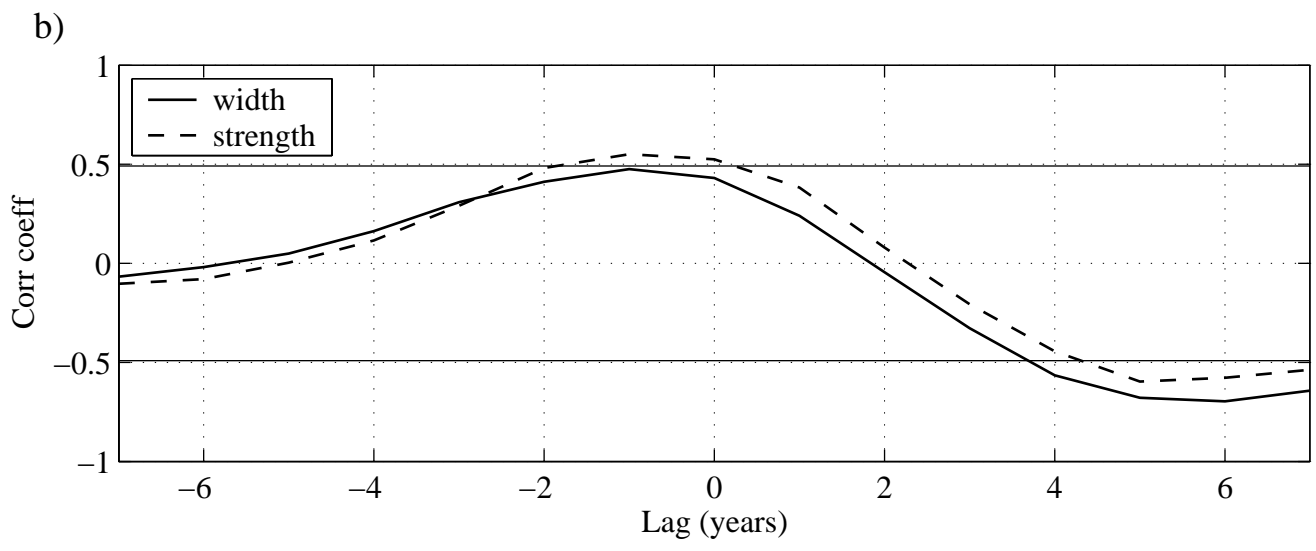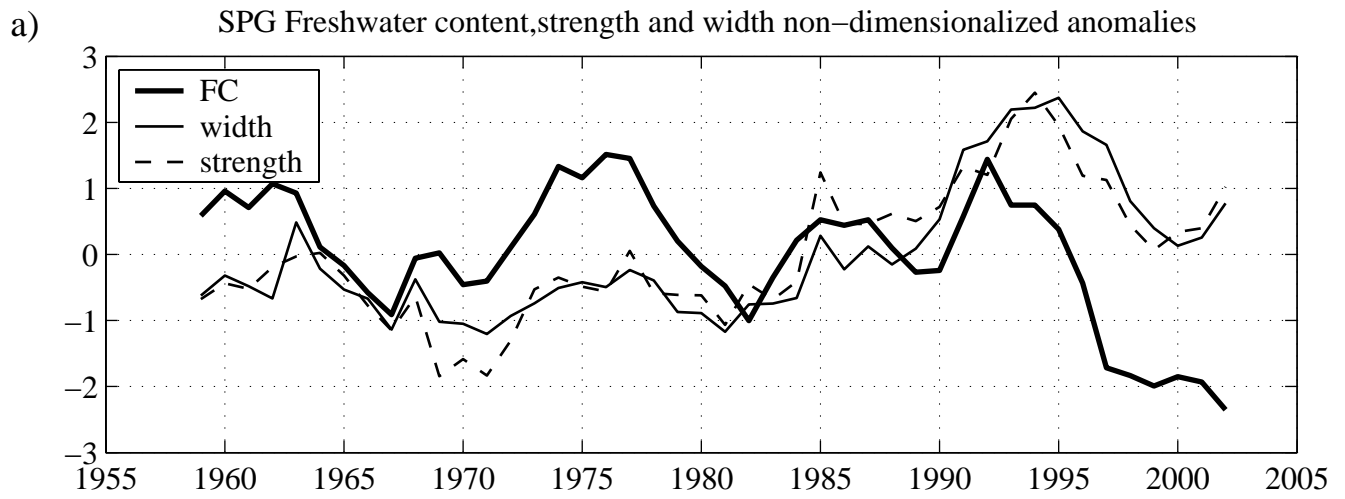a) Mean 1960–02   b) Mean 1968–72   c) Mean 1983–87   d) Mean 1993–97
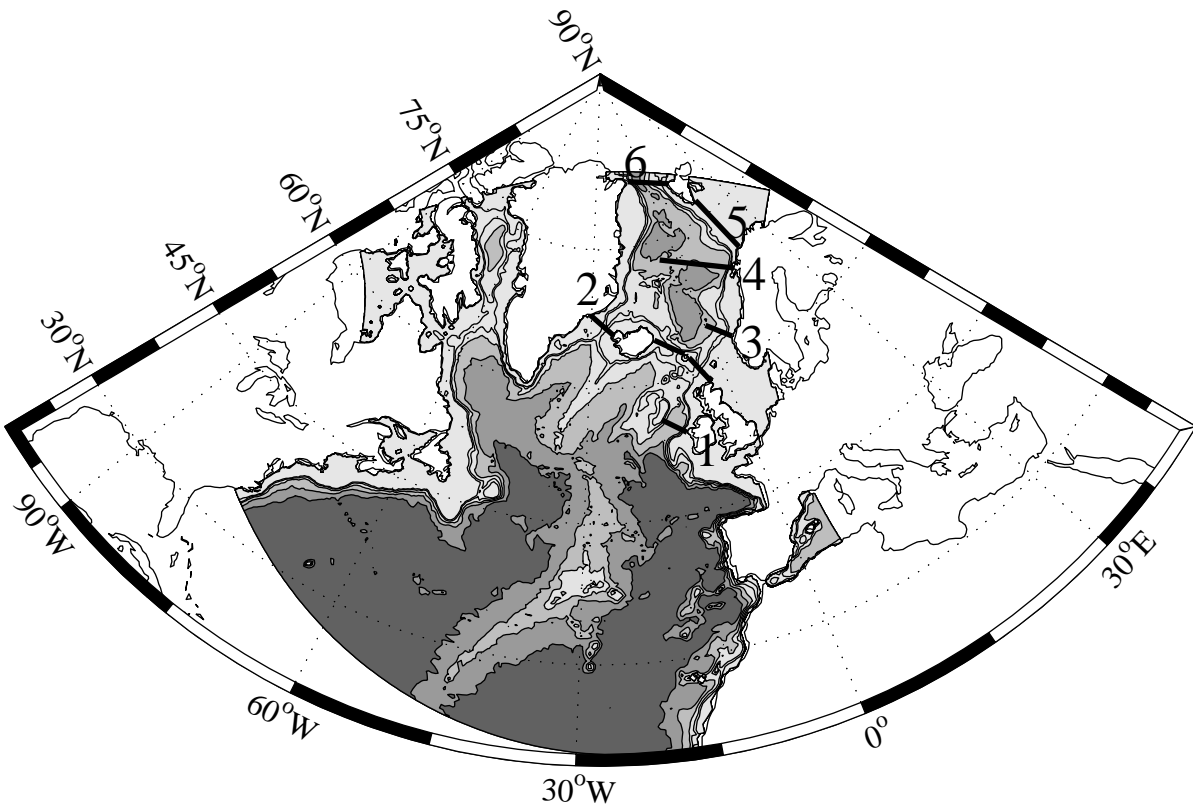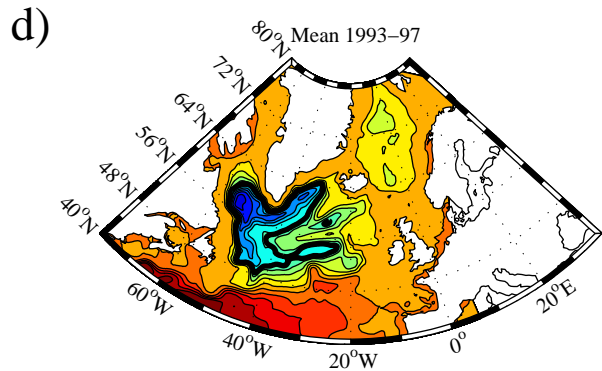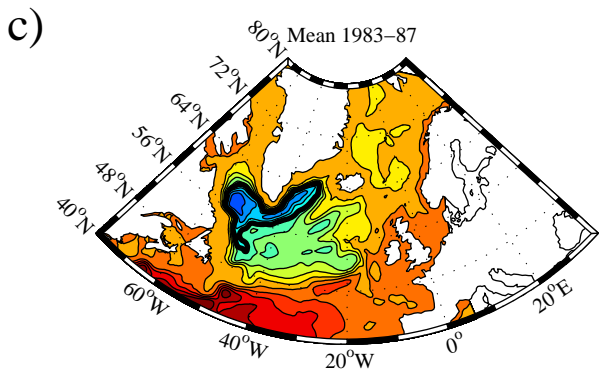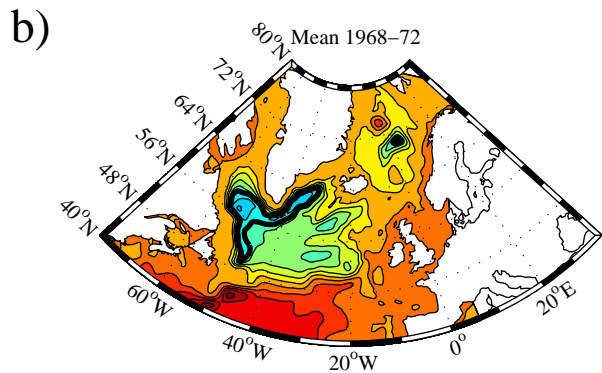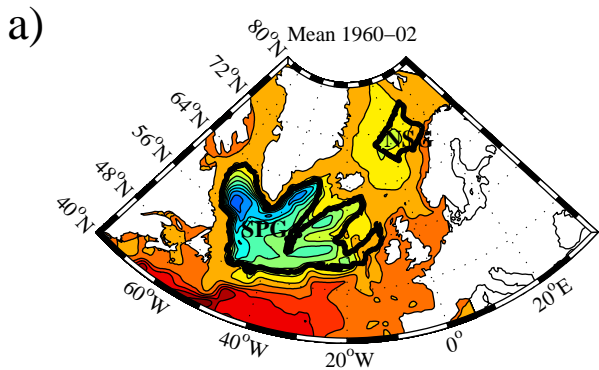
Freshwater content Subpolar Gyre

Volume flux across Greenland–Scotland Ridge

a) Mean SPG density, salinity and temperature non−dimensionalized anomalies

a) SPG Freshwater content,strength and width non−dimensionalized anomalies

a) NAO and SPG Freshwater content & strength
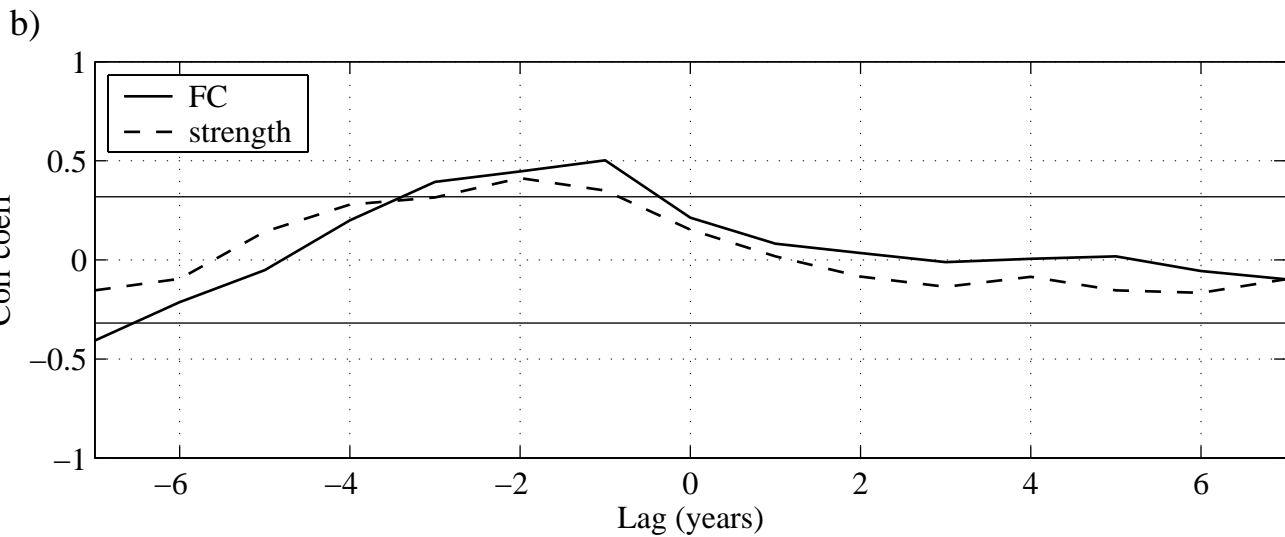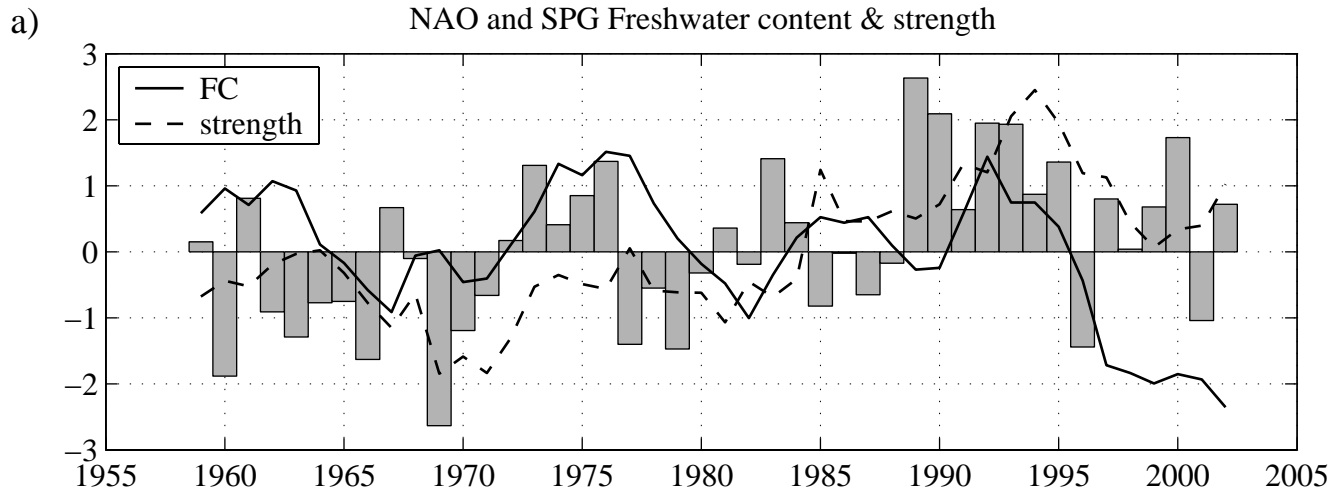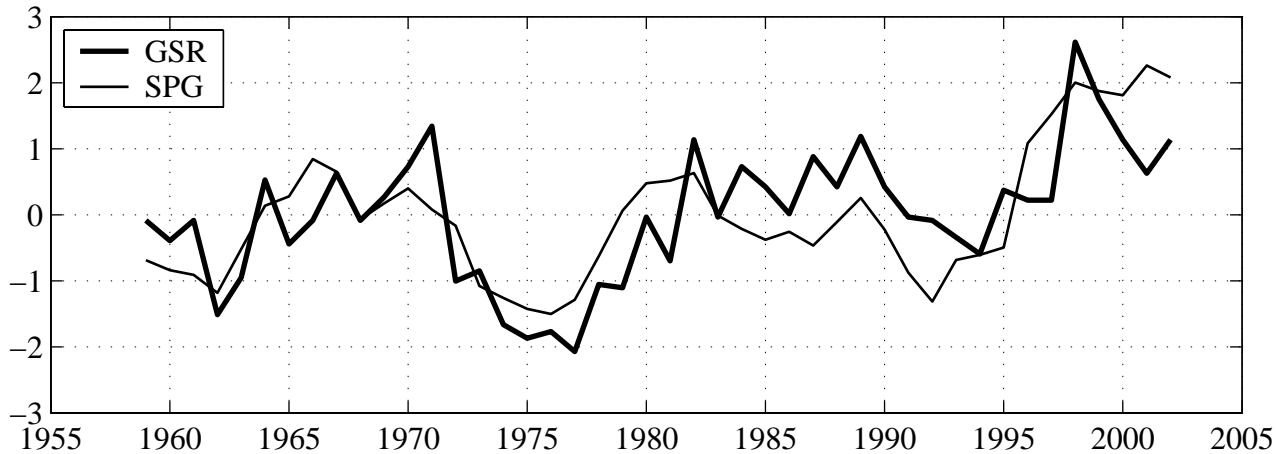
a) Non−dimensionalized mean salinity anomalies in GSR inflow and SPG

a) Mean ρ ,S and T non−dimensionalized anomalies in GSR inflow

b)

a)

GSR Atlantic inflow,mean S and mean T non−dimensionalized anomalies

b)

a) NAO and GSR non−dimensionalized volume flux anomalies

b)